LOW-PRESSURE REVERSIBLE AXIAL FAN WITH STRAIGHT PROFILE BLADES AND RELATIVELY HIGH EFFICIENCY

by

***Živan T. SPASIĆ*[a*], *Saša M. MILANOVIĆ*[a], *Vanja M. ŠUŠTERŠIČ*[b], *and Boban D. NIKOLIĆ*[a]**

[a] Faculty of Mechanical Engineering, University of Niš, Niš, Serbia
[b] Faculty of Engineering, University of Kragujevac, Kragujevac, Serbia

Original scientific paper
DOI: 10.2298/TSCI120503194S

The paper presents the design and operating characteristics of a model of reversible axial fan with only one impeller, whose reversibility is achieved by changing the direction of rotation. The fan is designed for the purpose of providing alternating air circulation in wood dryers in order to reduce the consumption of electricity for the fan and increase energy efficiency of the entire dryer. To satisfy the reversibility of flow, the shape of the blade profile is symmetrical along the longitudinal and transversal axes of the profile. The fan is designed with equal specific work of all elementary stages, using the method of lift forces. The impeller blades have straight mean line profiles. The shape of the blade profile was adopted after the numerical simulations were carried out and high efficiency was achieved. Based on the calculation and conducted numerical simulations, a physical model of the fan was created and tested on a standard test rig, with air loading at the suction side of the fan. The operating characteristics are shown for different blade angles. The obtained maximum efficiency was around 0.65, which represents a rather high value for axial fans with straight profile blades.

Key words: *reversible axial fan, dryers, profile, characteristics, efficiency experiment*

Introduction

Reversible axial fans are used to achieve forced air-gas flow in the primary and reverse flow regime. Efficiency of these fans is relatively low for the straight profile of the blades and attack air flow on the profiles.

Type VKS dryers for drying timber (manufacturer "Nigos electronik", Niš) use low-pressure axial fans for providing alternating air circulation, fig. 1. Depending on the drying capacity, the number of fans which are mounted under the ceiling of the drying chamber range from 3 to 8, for whose drive the power of 5 to 24 kW is required. Electrical power of fans is around 0.2-0.3 kW/m^3 of timber. By adequate construction of the fan and increase in fan efficiency, the drive power for the fan can be reduced. The efficiency of reversible axial fans that are now being used is about 0.58.

* Corresponding author; e-mail: zivans@masfak.ni.ac.rs

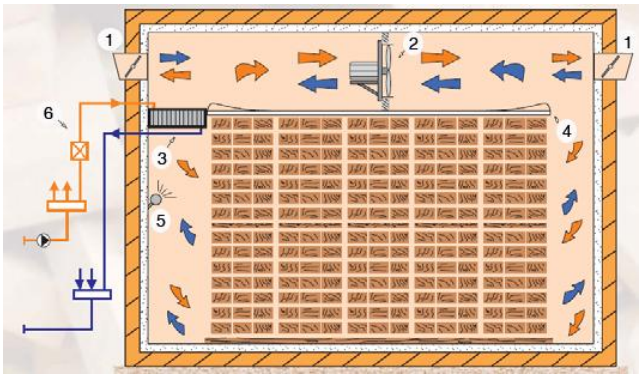

Figure 1. Timber dryer – type VKS;
1 – Servo-controlled flaps,
2 – Reversible axial fans, 3 – Heaters,
4 – False – ceiling, 5 – Atomizers,
6 – Substation

To increase the energy efficiency of a dryer, the design of a reversible axial fan was developed and tested on the test rig.

Calculation of the model fan

The efficiency of the fan depends on the shapes of the blade profiles, the blade itself, and the ratio of the diameters of the impeller hub and the shroud.

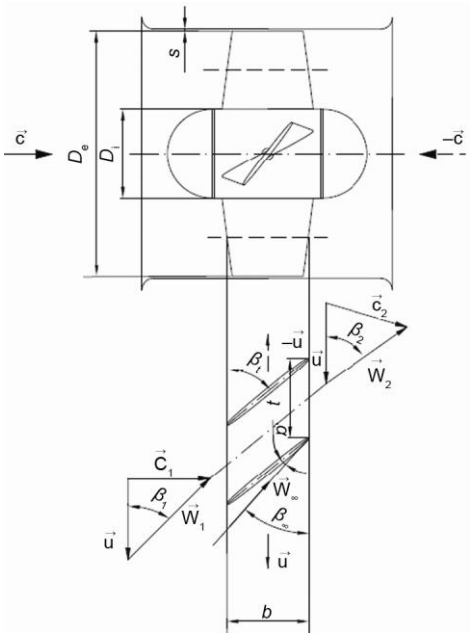

Figure 2. Reversible axial fan

To determine the shape of the impeller blade, it is sufficient to determine its profiles in 5 to 12 elementary stages, approximately equally distributed along the height of the blade. Figure 2 schematically shows a meridian section of a reversible axial fan, with a developed cylindrical section for the mean section of the impeller, and velocity triangles immediately before and after the cascade. The velocity triangles are shown for the primary flow of the fluid, left-to-right flow (fig. 1: flow velocity $\vec{c}$, circumferential velocity direction $\vec{u}$). With the change in the flow direction (circumferential velocity direction $-\vec{u}$), the flow becomes reversible (flow velocity $-\vec{c}$).

The fan impeller is designed under the principle of equal specific work of all elementary stages, that is, under the principle of flow along axially symmetrical cylindrical surfaces.

For calculation parameters, volumetric flow $Q = 3.61$ m^3/s, total pressure rise $\Delta p_{tot} = 180$ Pa, rotation speed $n = 1405$ rpm, and assumed efficiency (hydraulic $\eta_h = 0.75$ and total $\eta = 0.65$), the basic geometry of the fan impeller was obtained [1, 2]:

- $D_i = 300$ mm – diameter of the fan impeller hub,
- $D_e = 630$ mm – peripheral diameter of the fan impeller, and
- $z_K = 6$ – number of impeller blades.

The diameter of the fan impeller hub and other geometrical values were obtained according to the recommendations for optimal values of dimensionless volume coefficient and pressure coefficient [3].

The fan was calculated with constant specific work in elementary stages ($Y_{K.i}$ = Y_K = const.), with straight mean line profiles with seven cylindrical sections equally distributed along the height of the blade. The calculation was performed using the method of lift forces with the expression:

$$\zeta_{YR}\frac{l}{t}=\frac{2\Delta w_u}{w_\infty} \tag{1}$$

For a necessary flow deflection that should be achieved by the profile cascade (ζ_{YR}), the coefficient of profile lift (ζ_Y) is determined for the appropriate incidence angle (α), as well as the angle of the profile inclination in the cascade (β_t) that will allow for flow deflection, fig. 2:

$$\beta_t=\beta_\infty+\alpha \tag{2}$$

where β_∞ is the angle of the mean relative velocity to infinity.

The lift coefficient of the individual profile is different than the lift coefficient of a profile in the cascade due to the presence of adjacent profiles. The relation between the lift coefficient of the profiles in the cascade (ζ_{YR}) and the individual profile (ζ_Y) is indicated with k (k = ζ_{YR}/ζ_Y) and it can be determined from the diagram (fig. 3), depending on the relative cascade pitch (t/l) and profile inclination angle β_t, where the values for the angles of the mean relative velocity to infinity β_∞. can be adopted in the first approximation.

As the lift coefficients for straight, completely symmetrical profiles are not known, the lift coefficients for a flat plate are used in the calculation of the lift coefficients (ζ_Y) of the individual profile. The lift coefficients (ζ_Y) for a flat plate can be determined theoretically (for frictionless flow) depending on the incidence angle (α):

$$\zeta_Y=2\pi\sin\alpha \tag{3}$$

or by using the diagram, obtained experimentally for round-arch profiles and flat plates [3, 4], shown in fig. 4, depending on the profile finesse (f/l), where the values for the flat plate are given along the ordinate, as a boundary case of the round arch f/l = 0 (l/R = 0).

Selection of straight symmetrical profiles for blade construction

The shape of the profile for blade construction was selected after the numerical simulations of flow were carried out in the fan with blades with straight, completely symmetrical profiles, and different distribution of thickness along the mean line of the profile and different curvatures of profile ends [1, 2]. After the analysis of the operating characteristics of fans obtained through numerical simulations, the straight profile (fig. 5) marked PP2 [2], was selected for blade construction, with the maximum thickness in the middle of the profile, at the hub δ_{imax} = 12 mm and at the shroud δ_{emax} = 6 mm, with the distribution of the thickness along the mean line as shown in tab. 1, and the profile leading and tail curvature radii r = r_1 = r_2 = 0.2δ_{max}.

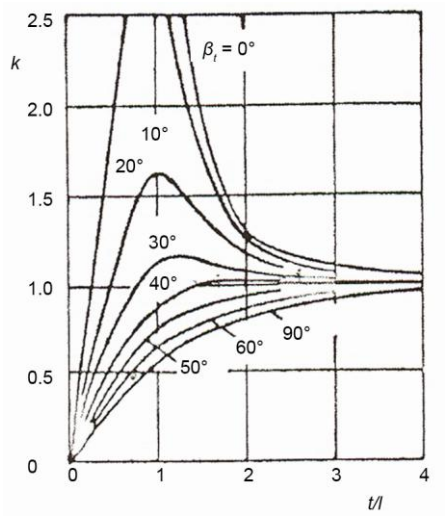

Figure 3. Values for k, $k = \zeta_{YR}/\zeta_Y$

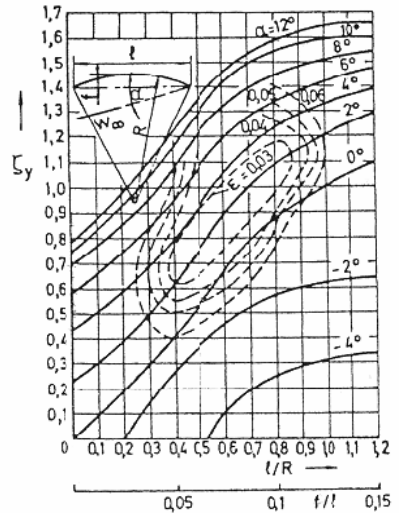

Figure 4. Lift coefficients of round-arch profiles ($l/R = 0 \Rightarrow$ flat plate)

Table 1. Distribution of thickness along the PP2 profile mean line

x_j/δ_j [$\cdot 10^{-2}$]	0.0	2.14	3.57	5.62	10.53	20.43	30.24	40.14	50	59.77	69.58	79.48	89.38	94.29	96.52	97.86	10.0
δ_j/δ_{jmax} [$\cdot 10^{-2}$]	0.0	43.33	50.0	58.33	73.33	86.67	95.00	96.67	100	96.67	95.00	86.67	73.33	58.33	50.00	43.33	0.0

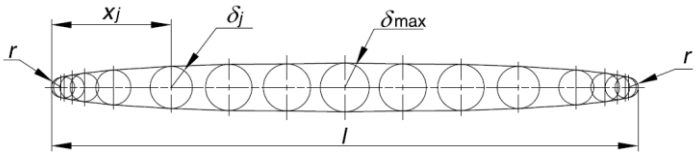

Figure 5. Geometry of the straight symmetrical profile, PP2

The basic data on geometry of the profile cascade in cylindrical sections i (i = I-VII), upon which the model of the fan for numerical simulations was formed, are given in tab. 2.

The difference in the inclination angles of the profile mean line at the hub (β_{ti} = 53.7°) and the shroud (β_{te} = 24.6°), the angular spatial blade curvature $\Delta\beta_L$ (fig. 6), is $\Delta\beta_{L.} = \Delta\beta_t = \beta_{ti.} - \beta_{te.} = 53.7 - 24.6 = 29.1°$.

Table 2. Geometry of profile cascade in cylindrical sections

Section: i	r_i [mm]	t_i [mm]	l_i [mm]	β_{ti} [°]	δ_{maxi} [mm]	$(\delta_{max}/l)_i$ [–]	r [mm]
I	150	157	144	53.7	12	0.083	2.4
II	178	186	138	42.3	11	0.080	2.2
III	205	215	133	36.4	10	0.075	2.0
IV	233	243	126	31.8	9	0.071	1.8
V	260	272	121	28.5	8	0.066	1.6
VI	288	301	114	26.0	7	0.061	1.4
VII	315	330	108	24.6	6	0.056	1.2

Model of the reversible axial fan for experimental testing

For the manufacture of a physical model for experimental research, apart from the calculated profiles for the formation of a numerical model (seven cylindrical impeller sections, tab. 2), for the purpose of better accuracy in constructing a spatially curved blade, the profiles for six more sections were calculated and defined, with the additional sections selected in the middle of the primary sections (marked with "prim" in tab. 3), thus the blade construction was performed with known profiles (PP2) for thirteen cylindrical sections of the impeller (13 elementary stages). The basic data for all cylindrical sections are given in tab. 3.

Figure 7(b) shows straight blade profiles developed in a plane (stacked profiles), whose mean lines developed in a plane are shown in fig. 7(a), while the data on the profile geometry (PP2 profile) are given in tab. 1.

Based on the calculations and technical documentation of the profile (2-D), the 3-D model of the fan blades was created in SolidWorks. On the basis of the 3-D drawings of the blade, a physical model of the blade was constructed from aluminium on a CNC milling machine (fig. 8), which was used to cast model fan blades.

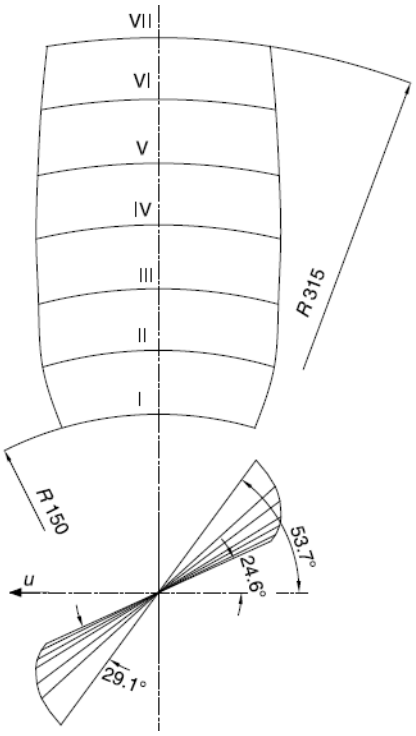

Figure 6. Blade with straight mean lines profile developed in a plane, $\Delta\beta_L = 29.1°$

Table 3. Geometry of profile cascade in cylindrical sections

Section: i	r_i [mm]	t_i [mm]	l_i [mm]	β_{ti} [°]	δ_{maxi} [mm]	δ_{maxi}/l_i [–]	$r_{1,2}$ [mm]
I	150	157	144	53.7	12.0	0.083	2.40
I'	164	172	141	47.6	11.5	0.082	2.30
II	178	186	138	42.3	11.0	0.080	2.20
II'	191	200	136	39.2	10.5	0.077	2.10
III	205	215	133	36.4	10.0	0.075	2.00
III'	219	229	129	34.1	9.5	0.074	1.90
IV	233	244	126	31.8	9.0	0.071	1.80
IV'	246	258	123	30.0	8.5	0.069	1.70
V	260	272	121	28.5	8.0	0.066	1.60
V'	274	287	117	27.0	7.5	0.064	1.50
VI	288	302	114	26.0	7.0	0.062	1.40
VI'	301	315	110	25.2	6.5	0.059	1.30
VII	315	330	108	24.6	6.0	0.056	1.20

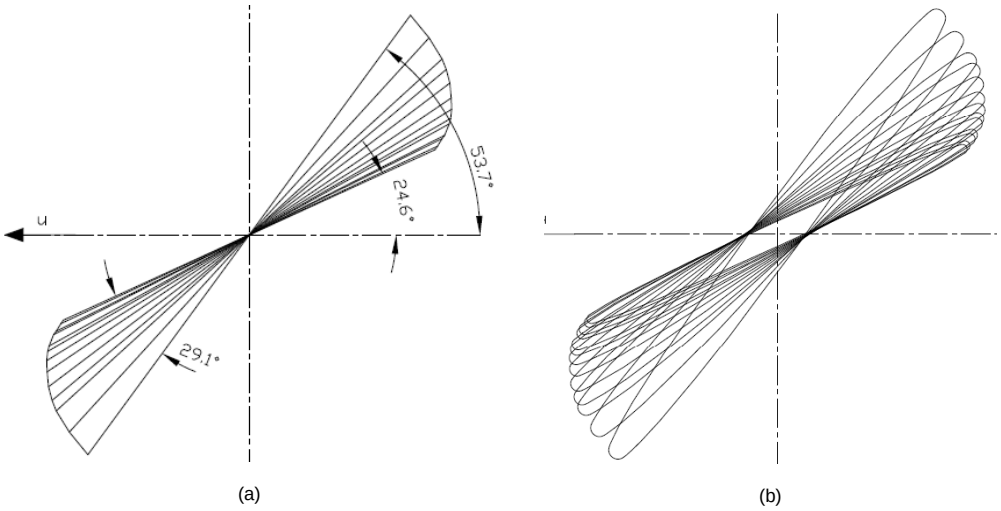

Figure 7. (a) Profile mean lines developed in a plane, (b) Blade profiles developed in a plane

Figure 8. Manufacturing the blade model on the CNC milling machine

On the basis of the blade model for casting, the blades of the model impeller were made from aluminium by sand casting. The impeller (fig. 9) had six blades (z_K = 6), which were attached to the hub of the impeller using M12 nuts and special conical bolts which were partially cast into the blades so as to allow manual adjustment and rotation of blades for a specific angle. The rotation of the blade was limited by the length of the hub (L_H = 120 mm) and the cylindrical shape of the hub.

The blades were mounted on the hub under a specific blade angle (β_t), which was defined in accordance with the profile inclination angle at the hub ($\beta_L = \beta_{ti}$).

The impeller was positioned in the fan casing of diameter D_e' = 635 mm, with the clearance between the impeller and the casing s = 2.5 mm (fig. 10). The electric motor was positioned inside a half cylinder of the same diameter as the impeller hub diameter (D_i = 300 mm), with a semi-spherical ending, which allowed for the flow around the electric motor and the hub with as small a loss as possible, ensuring the equal intake of the air flow into the impeller along the height of the blade, fig. 10(b).

Figure 9. Impeller with straight blade profiles (D_e = 630 mm, D_i = 300 mm, D_i/D_e = 0.476, z_K = 6)

(a) (a)

Figure 10. Appearance of the model fan: D_e = 630 mm, s = 2.5 mm, z_k = 6

Experimental testing

The testing and obtaining of the operating characteristics of the fan was conducted by air loading on the suction side of the fan, for a nominal rotation speed of the electric motor n = 1405 rpm [5, 6].

The testing was conducted on a standard test rig (AMCA 210), with the suction duct with the diameter D = 690 mm (fig. 11), in the Laboratory for Hydraulic and Pneumatic Testing of the Faculty of Mechanical Engineering in Niš (fig. 12).

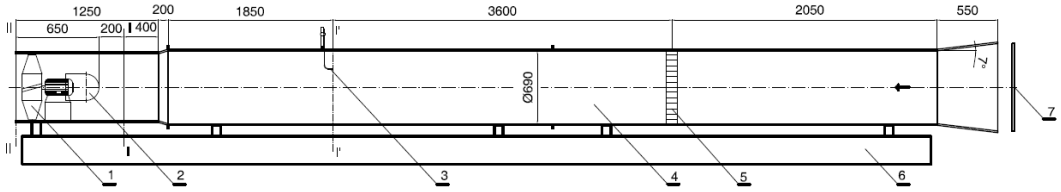

Figure 11. Test rig for testing axial flow fans

1 – Fan for testing, 2 – Deflector, 3 – Prandtl probe with traverse, 4 – Channel testing, 5 – Airflow straightener, 6 – Stand, I′-I′– Cross-section for measuring flow rate, I-I – Cross-section in front of the fan, II-II – Cross-section behind the fan

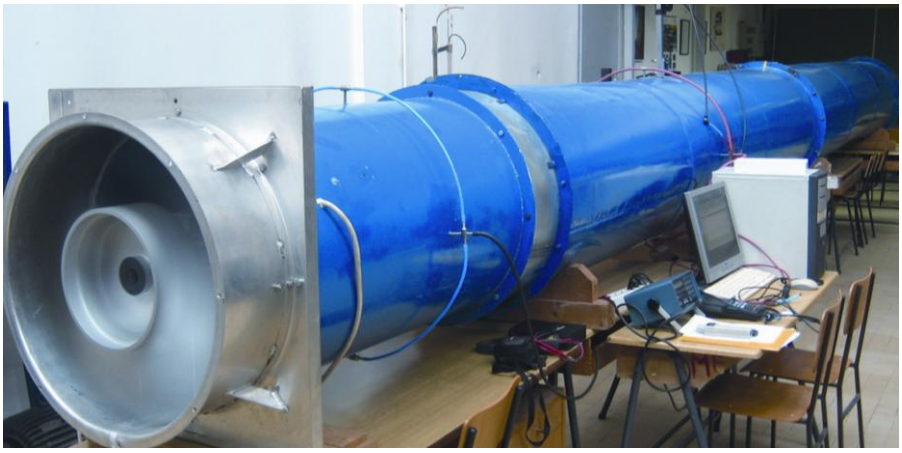

Figure 12. Photograph of the test rig with the part of the measuring equipment

Apart from measuring the pressure and determining the flow, the electrical magnitudes at the entry into the electric motor of the fan, and the rotation speed of the fan and air parameters in the laboratory (atmospheric pressure and temperature) were also measured [2, 5]. The power of the electric motor was P_M = 1.5 kW, the characteristics of which were known and are shown in fig. 13.

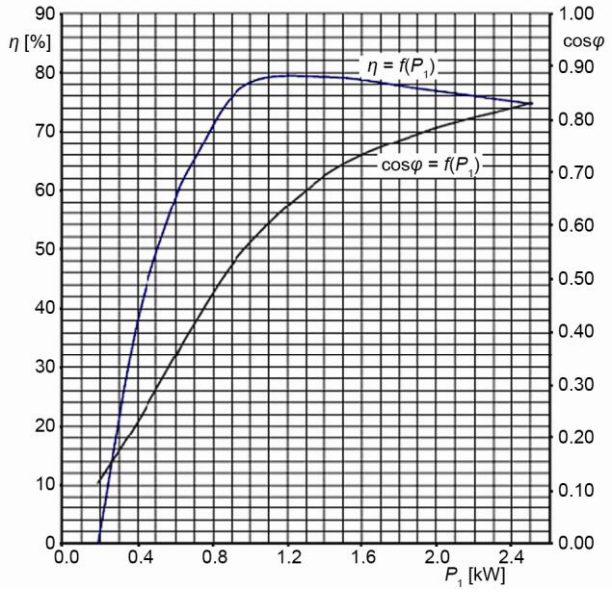

Figure 13. Efficiency of electric motors, $\eta = f(P_1)$ and $\cos\varphi = f(P_1)$

The volume flow rate was determined on the basis of the measured and mean pressure rate in the cross section I′-I′. The dynamic pressure was measured with the Prandtl probe in five points that were deployed on the defined radii [2, 6]. The total rise in the pressure in the fan was determined as the difference of total pressures behind (p_{IItot}) and in front of the fan (p_{Itot}):

$$\Delta p_{tot} = p_{IItot} - p_{Itot} \tag{4}$$

For testing the fan for suction and free air flow outlet into the atmosphere (fig 11), the total rise in the pressure in the fan equals the static pressure (vacuum) in the cross-section in front of the fan [3]:

$$\Delta p_{tot} = p_I^{(V)} \tag{5}$$

Static pressure in front of the fan was measured in the cross section I-I, using a piezometer ring, while static pressure behind the fan (cross section II-II) was considered as equal to the atmospheric pressure.

The efficiency of the electric motor is given in dependence of the input power of the electric motor P_1.

Measuring instruments

The characteristics of measuring instruments are given in tab. 4 to 7.

Table 4. Pressure

Instrument	Type	Accuracy	Range	Manufacturer
Manometer	MEDM 5K	±1% of v. reading	(0-5000) Pa	BSRIA
Manometer	TESTO 350	±0.5% v. reading	(0-100) hPa	Testo

Table 5. Rotation speed

Instrument	Type	Accuracy	Range	Manufacturer
Tachometer	digital	±0.04%±2	(1000-10000) rpm	Echtech

Table 6. Electrical magnitude (voltage, current and power)

Instrument	Type	Accuracy	Range	Manufacturer
Univ. clamp-on millimeter	M5110	±2% of v.read.	*U*>130V, *I*<150A	ABB
Portable power analyzer	Circutor AR5-L	1% ±2 dec.	*U*>100V, *I*<200A	Circutor

Table 7. Atmospheric pressure and temperature

Instrument	Type	Accuracy	Range	Manufacturer
Barometer	Manometer	1.0%	(890-1060) mbar	GDR
Thermometer	with mercury	0.5%	0-50 °C	TGL

Results of the experimental testing

For the region of the stable performance of the fan, the diagrams of operating characteristics of the fan are shown, total pressure rise $\Delta p_{tot}(Q)$ (fig. 14), power $P(Q)$ and efficiency $\eta(Q)$ (fig. 15), obtained on the test rig for different various impeller blades angle (β_L). Using the theory of similarity, the fan characteristics were calculated and shown for a constant rotation speed of the fan n = 1405 rpm and air density ρ = 1.2 kg/m^3.

The model of the fan was tested for three positions of impeller blade angle (β_L) measured at the hub: β_L = 52.5°, β_L = 55°, and β_L = 57.5°.

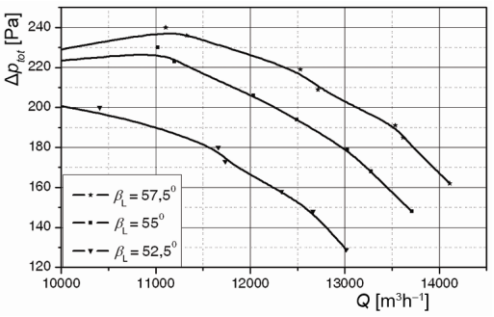

Figure 14. Total pressure rise of the fan, $\Delta p_{tot}(Q)$

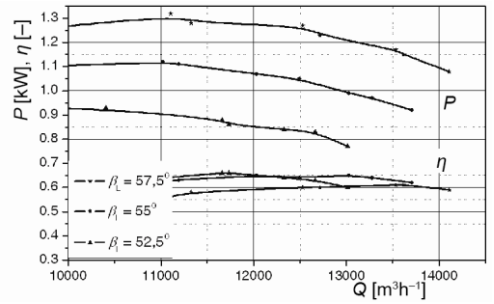

Figure 15. Power and efficiency characteristics, $P(Q)$ and $\eta(Q)$

The fan achieved the optimal operating parameters (maximum value of efficiency) for position:

– impeller blade angle $\beta_L = 52.5°$: $\Delta p_{tot} = 175$ Pa, $Q = 11700$ m^3/h, $P = 0.86$ kW, $\eta = 0.66$
– impeller blade angle $\beta_L = 55°$: $\Delta p_{tot} = 179$ Pa, $Q = 13000$ m^3/h, $P = 1.00$ kW, $\eta = 0.65$, and
– impeller blade angle $\beta_L = 57.5°$: $\Delta p_{tot} = 186$ Pa, $Q = 13600$ m^3/h, $P = 1.15$ kW, $\eta = 0.61$.

Conclusions

The calculation flow parameters ($\Delta p_{tot} = 180$ Pa, $Q = 13000$ m^3/h), for the nominal rotation speed of the electric motor ($n = 1405$ rpm), with straight blade profiles (PP2 profiles), were achieved for the position impeller blade angle of $\beta_L = 55°$ and fan efficiency of $\eta = 0.65$.

The fan efficiency of $\eta = 0.66$ was obtained for the impeller blade angle of $\beta_L = 55°$. The achieved efficiency is high for reversible axial fans with straight blade profiles. This shows that the blade profiles were calculated well, and that the obtained impeller with straight blade profiles is energy efficient.

The efficiency of the designed fan is 12% higher than for the fans that have thus far been used in dryers, which will reflect directly on the efficiency of the entire dryer.

By using the designed fans, the electricity needed to drive the fans is reduced to 0.18-0.27 kW/m^3 of timber.

Nomenclature

b – cascade width, [m]
D – diameter, [m]
l – profile length, [m]
n – rotation speed, [rpm]
P – power, [W]
Q – flow, [m^{3}s^{-1}]
s – tip clearance, [m]
t – cascade pitch, [m]
w – relative velocity, [ms^{-1}]

Greek symbols

α – incidence angle, [°]
β_L – impeller blade angle [°]
δ – thickness profile,[m]
Δp_{tot} – total pressure rise, [Pa]
η – efficiency, [–]
ζ_Y – lift coefficient, [–]

Subscripts

1, 2– inlet and outlet
∞ – infinity
t – mean line
e – periphery
i – for hub, cylindrical sections
L – blade

References

[1] Bogdanović, B., *et al*., The Development Construction of Reversible Axial Fans (in Serbian), Report for project No. 18012, funded by the Serbian Ministry of Education, Science and Technological Development, the period: 31.04.2008–31.04.2011
[2] Spasić, Ž., Numerical and Experimental Investigation of the Influence of the Blade Profile Shape on the Reversible Axial Fan Characteristics (in Serbian), Ph. D. thesis, Faculty of Mechanical Engineering, University of Nis, Nis, Serbia, 2012
[3] Eck, B., *Fans-Design and Operation of Centrifugal, Axial-Flow and Cross-Flow Fans,* Pergamont Press, Oxford, England, 1973
[4] Krsmanović, Lj., Gajić, A., *Turbomachinery – Fans* (in Serbian), Faculty of Mechanical Engineering, University of Belgrade, Belgrade, 2000
[5] Spasić, Ž., Bogdanović, B., Radić, M., Variation of Operation of Low-Pressure Reversible Axial Fans Driven by Induction Motor from Start to the Steady-State, *Proceedings on CD* (SIMTERM 2011, Sokobanja, 2011, pp. 586-595
[6] Bogdanović, B., Milenković, D., Bogdanović-Jovanović, J., Fans-Performance and Operating Characteristics (in Serbian), Faculty of Mechanical Engineering, University of Nis, Nis, Serbia, 2012

Paper submitted: May 3, 2012
Paper revised: September 20, 2012
Paper accepted: September 25, 2012